ELSEVIER

Polymer 43 (2002) 3247–3255

polymer

www.elsevier.com/locate/polymer

Rheological behavior of multiwalled carbon nanotube/polycarbonate composites

Petra Pötschke*,[1], T.D. Fornes, D.R. Paul

Department of Chemical Engineering and Texas Material Institute, Center for Polymer Research, University of Texas at Austin, Austin, TX 78712-1062, USA

Received 29 November 2001; received in revised form 1 February 2002; accepted 5 February 2002

Abstract

The rheological behavior of compression molded mixtures of polycarbonate containing between 0.5 and 15 wt% carbon nanotubes was investigated using oscillatory rheometry at 260 °C. The nanotubes have diameters between 10 and 15 nm and lengths ranging from 1 to 10 μm. The composites were obtained by diluting a masterbatch containing 15 wt% nanotubes using a twin-screw extruder. The increase in viscosity associated with the addition of nanotubes is much higher than viscosity changes reported for carbon nanofibers having larger diameters and for carbon black composites; this can be explained by the higher aspect ratio of the nanotubes. The viscosity increase is accompanied by an increase in the elastic melt properties, represented by the storage modulus G', which is much higher than the increase in the loss modulus G''. The viscosity curves above 2 wt% nanotubes exhibit a larger decrease with frequency than samples containing lower nanotube loadings. Composites containing more than 2 wt% nanotubes exhibit non-Newtonian behavior at lower frequencies. A step increase at approximately 2 wt% nanotubes was observed in the viscosity–composition curves at low frequencies. This step change may be regarded as a rheological threshold. Ultimately, the rheological threshold coincides with the electrical conductivity percolation threshold which was found to be between 1 and 2 wt% nanotubes.

Keywords: Carbon nanotube composites; Rheological behavior; Electrical conductivity

1. Introduction

Composites of carbon nanotubes (CNTs) in polymeric matrices have attracted considerable attention in the research and industrial communities due to their unique mechanical and electrical properties. CNT polymer nanocomposites possess high stiffness, high strength, and good electrical conductivity at relatively low concentrations of CNT filler [1–9].[2] These enhancements ultimately stem from the distinct properties of the CNTs themselves. For example, various studies involving singlewalled nanotubes (SWNT) and multiwalled nanotubes (MWNT) have demonstrated that CNT can have moduli and strength levels in the range 200–1000 GPa and 200–900 MPa, respectively [10–12]. Other studies have shown that CNTs have diverse electrical properties, capable of acting as metallic-like conductors or having characteristics of a semiconductor depending upon the distortion or 'chirality' of the graphite lattice [13,14]. In addition, CNTs have very large aspect ratios (length to diameter ratio), as high as 100–1000 [1].[2] Such special properties make CNTs excellent candidates for high strength and electronically conductive, polymer composite applications.

Currently, there are two major areas in which CNTs are being used, electronics and automotive. In electronic applications, particularly in the semiconductor field, CNTs are used to dissipate unwanted static charge build-up. This dissipative effect is achieved by thoroughly dispersing CNTs in the polymeric material such that an interconnecting structure of CNT is formed. This interconnecting network thus provides a conductive pathway for charge to flow. Conductive compounds need very low fibril loadings, typically less than 5 wt% to achieve electrostatic dissipation, compared to about 8–20 wt% for carbon black-based compounds. These different loading levels offer many advantages. In the automotive industry, CNTs are used as a conducting agent to aid in electrostatic painting. Such parts are produced by melt processing. A key issue in producing superior CNT nanocomposites applications is the

* Corresponding author. Tel.: +49-351-4658395; fax: +49-351-4658565.

E-mail addresses: poe@ipfdd.de (P. Pötschke), drp@che.utexas.edu (D.R. Paul).

[1] Permanent address: Institute of Polymer Research Dresden, Hohe Strasse 6, D-01069 Dresden, Germany. Tel.: +49-351-4658395; fax: +49-351-4658565.

[2] www.fibrils.com, www.fibrils.com/grafibs.htm (accessed September 2001).

0032-3861/02/$ - see front matter
PII: S0032-3861(02)00151-9

ability to control dispersion of the CNT in polymeric matrices. This, however, hinges on an in-depth understanding of CNT–polymer nanocomposite rheology, a topic that has not received much attention.

Presently, three methods are commonly used to incorporate nanotubes into polymers: (i) film casting of suspensions of nanotubes in dissolved polymers, (ii) polymerization of nanotube–polymer monomer mixtures, and (iii) melt mixing of nanotubes with polymers. In most fundamental studies, film casting was used to investigate the properties of polymers containing CNTs including the effects of nanotube dispersion and orientation [8,15,16], deformation mechanisms [8,17] and interfacial bonding [8,17]. Mechanical properties [8], dynamic-mechanical properties [18], and electrical conductivity [18,19] have also been investigated. Raman spectroscopy has been used to obtain information on interactions between nanotubes and the polymer matrices [8,16,20]. Orientation and degree of alignment have been studied by X-ray diffraction [15]. Film casting has often been the only processing option used owing to limited availability of CNTs and/or their high cost.

Studies using melt processed thermoplastic polymer/CNT nanocomposites have been quite limited. On the other hand, melt processing is the preferred method of composite formation in many cases. The tendency of nanotubes to form aggregates may be minimized by appropriate application of shear during melt mixing.[2] For example, Haggenmueller et al. [2] applied a combined solvent casting and melt processing procedure to produce films of poly(methyl methacrylate) (PMMA) containing SWNT. They pressed small pieces of cast films between heated plates, then broke the resulting film again into small pieces, and repeated the procedure many times. The films obtained by this melt processing technique had a more homogeneous nanotube distribution than the cast film and led to much better mechanical properties. Jin et al. [5] used a miniature mixer-molder (ATLAS) to produce small quantities (ca. 0.4 g) of well-dispersed mixtures of MWNT in PMMA. The well-dispersed mixtures were then compressed into thin films to investigate their dynamic-mechanical behavior; a significant increase in the storage modulus was observed. Lozano et al. [3,4] used a Haake miniature laboratory mixer (14–20 g) to disperse vapor grown carbon fibers in polypropylene (PP). After compression molding into thin films they investigated the dispersion, melt rheology, conductivity, mechanical and dynamic-mechanical properties, and the influence of the nanotube fibrils on the PP crystallization behavior. Ferguson et al. [7] reported on kilogram quantities of polycarbonate-based nanotube formulations produced in a Buss Kneader. They compared formulations obtained by mixing of a diluted masterbatch with different amounts of reprocessed compounds. The reprocessing in a Buss Kneader led to better dispersion of the fibrils resulting in increased conductivity.

To our knowledge, there are no reports on the melt rheological behavior of MWNT filled polymers. On the other hand, Lozano and Barrera [3] have studied the melt rheological properties of carbon fiber filled thermoplastic polymers. The vapor grown carbon fibers used in these investigations are treated as a model system for SWNT and MWNT. These fibers were similar in length as the MWNT, but their diameters were about 10 times larger than the MWNT used in the present study. Therefore, the results may not be directly comparable to the rheological behavior of SWNT or MWNT composites.

The purpose of this paper is to examine the rheological properties of MWNT filled polycarbonate nanocomposites formed by melt extrusion. The influence of nanotube content on complex viscosity, storage modulus and loss modulus are examined. Rheological behavior at high frequencies is used to estimate the effect of the filler on processing properties; however, the normal Cox–Merz rule relating complex viscosity to steady shear viscosity can break down in complex systems like composites [21]. Low frequency behavior is sensitive to the structure of the composites and can be used to obtain information about the percolation state of the MWNT within the composite. The materials are also characterized by scanning electron microscopy (SEM) and electrical resistivity measurements. An attempt is made to connect the morphological and resistivity information with rheological observations.

2. Experimental

2.1. Materials and characterization

A masterbatch of 15 wt% carbon MWNT in polycarbonate (PC/CNT) was obtained from Hyperion Catalysis International, Cambridge, MA. The nanotubes are vapor grown and typically consist of 8–15 graphitic layers wrapped around a hollow 5 nm core.[2] They are produced as agglomerates and exist as curved intertwined entanglements [22,23]. Typical diameters range from 10 to 15 nm, while lengths are between 1 and 10 μm. The density is approximately 1.75 g/cm^3 [18]; a surface area of 250 m^2/g was determined by the BET method.[2] The masterbatch was compounded using a MDK 46 Buss Kneader (L/D = 11/1), according to reports from Hyperion [7], and was delivered in pellet form. The masterbatch was diluted with a polycarbonate supplied by Mitsubishi Engineering Plastics with the commercial designation of Iupilon E-2000. In addition, a masterbatch of 20 wt% MWNT in polyamide-6 (PA/CNT), also obtained from Hyperion, was used for comparative purposes in the SEM investigations.

2.2. Nanocomposite preparation

The materials were dried for a minimum of 16 h at 80 °C in a vacuum oven. One-kilogram mixtures of polycarbonate with the masterbatch were extruded using a Haake co-rotating, intermeshing twin-screw extruder (length D = 30 mm, L/D = 10) to obtain concentrations of 0.5, 1, 2, and 5 wt%

nanotubes in polycarbonate. According to the material densities (1.20 g/cm^3 for PC[2] and 1.75 g/cm^3 for CNT [18]), the corresponding volume concentrations are 0.34, 0.68, 1.37, and 3.40 vol%. The screw design has been described previously [24]. Compounding was carried out using a barrel temperature of 240 °C, a screw speed of 280 rpm, and a feed rate of 980 g/h. Polycarbonate compounds were compression molded into $65 \times 13 \times 3$ mm^3 bars.

2.3. Electrical resistivity measurements

The volume resistivity of compression molded bars were determined by measuring the DC resistance along the length direction through bars approximately 40 mm in length. A Keithley electrometer Model 6517 with a 8002A High Resistance Test Fixture was used to measure the high resistance samples. Special clamps were designed for holding the injection molded bars. Instrument control, data acquisition and evaluation were performed by means of an application software, which was self-developed using the 'Testpoint' software kit of Keithley Instruments. This equipment allows resistivity measurements up to 10^{17} Ω. Different applied voltages were used on different samples, depending on the level of resistivity of the specimen. Highly conductive samples caused short-circuiting of the equipment when the applied voltage was too high. Thus, the voltage was adapted to the resistivity and was 500 V for PC and composites with up to 1 wt% CNT and 1 V for 2 wt% and greater CNT. The samples with 5 and 15 wt% were measured using a Keithley Model 2000 electrometer, which is more sensitive to lower resistivity levels. To ensure that volume resistivity did not reflect surface resistivity effects, thin sheets approximately 1 mm in thickness of the 2 wt% CNT composite were compression molded and tested for surface and volume resistance using a 8009 Resistivity Test Fixture equipped with ring electrodes. The surface resistivity results showed similar values as the volume results, thus indicating no significant surface resistivity effect. According to ASTM D4496 and D257, the resistivity was converted to volume resistivity, ρ_v, using the formula

$$\rho_v = WDR_v/L \quad (1)$$

where W is the width, D the thickness, L the length of the sample, and R_v is the measured resistance. The reported values represent the mean of 7–10 samples, where the standard deviation relative to the mean was less than 10%.

2.4. Rheological measurements

Prior to rheological measurements, compression molded bars were cut into $13 \times 13 \times 3$ mm^3 squares and dried at 80 °C for a minimum of 24 h under vacuum. Dynamic rheological measurements were performed using an advanced rheometric expansion system (ARES) rheometer from Rheometrics, Inc. The measurements were carried out in an oscillatory shear mode using a parallel plate geometry (25 mm diameter) at 260 °C under nitrogen atmosphere. Frequency sweeps between 0.1 and 100 rad/s were carried out at low strains (0.1–10%) which were shown to be within the linear elastic range for these materials. The upper limits of the viscoelastic range, determined in strain sweeps at 10 rad/s, were found to decrease with nanotube content. Repeated sweeps with increasing and decreasing frequencies showed that the material is stable under the measurement conditions. Specimens were placed between the preheated plates and were allowed to equilibrate for approximately 10 min prior to each frequency sweep run. The obtained values were corrected to the true volume between the plates.

2.5. Morphological characterization

A LEO 1530 scanning electron microscope was used to characterize composite morphology. Samples taken directly from the masterbatch were investigated by cutting pellets with a razor blade at room temperature which caused fracture; SEM images were made of the surface of the fractured region. SEM images were also made for cryofractured-compression molded bars formed from diluted mixtures. The samples were investigated with and without a sputtered coating.

In addition to SEM analysis, the nanocomposites were dissolved in tetrahydrofuran (THF) in an effort to assess the state of dispersion of the nanotubes. A small pellet of the masterbatch (8 mg, corresponding to 1.2 mg nanotubes) and corresponding weights of the diluted materials were immersed in approximately 50 ml of THF for about 2 weeks at room temperature. The solutions were formulated to have an equal amount of nanotubes in each vial. Under these conditions, polycarbonate is dissolved thereby leading to a suspension of the nanotubes in the solvent-PC solution.

3. Results

3.1. Electrical resistivity

Fig. 1 shows the effect of adding CNTs on volume resistivity. At very low concentrations of CNT, the resistivity gradually decreases with increasing nanotube content. However, at 2 wt%, a sizable reduction in resistivity, in the order of 10^{10} Ω cm, is observed. This stepwise change in resistivity is a result of the formation of an interconnected structure of CNTs and can be regarded as an electrical percolation threshold. This simply means that at concentrations between 1 and 2 wt% CNT, a very high percentage of electrons are permitted to flow through the sample due to the creation of an interconnecting conductive pathway. At concentrations above 2 wt% CNT, the volume resistivities are low and decrease marginally with increasing CNT content. It should be noted that the measured resistivity values in Fig. 1 were obtained using different applied

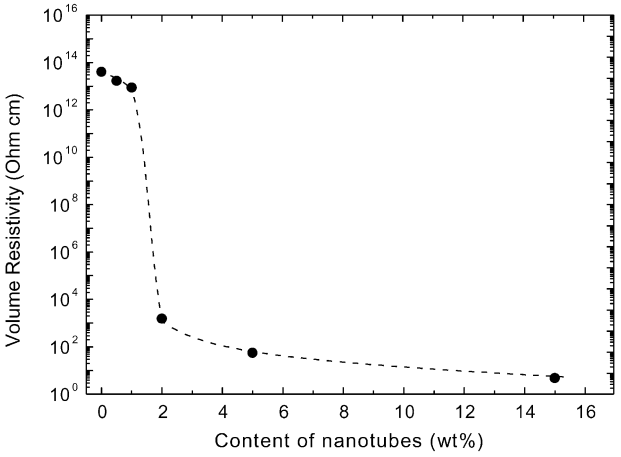

Fig. 1. Effect of CNT content on volume resistivity. Measurements were made with an applied voltage of 500 V for the high resistance materials (1 wt% or less) and 1 V for the more conductive materials (2 wt% or greater).

voltages, as mentioned in Section 2. Volume resistivity may show a dependence on the applied voltage. Therefore, the values presented in Fig. 1 may have been slightly different if the applied voltage was held constant, which was experimentally impossible using the different techniques employed here. In any case, this will not affect the concentration at which electrical percolation occurs. Interestingly, the measured values are in accordance with values given by Hagerstrom and Greene [6][2] who found a volume resistivity of 10^2 Ω cm for 5 wt% nanotubes in PC.

3.1. Rheological properties

The complex viscosities, $|\eta^*|$, of the nanotube masterbatch, the pure polycarbonate, and the diluted composites are shown in Fig. 2. The masterbatch, containing 15 wt% nanotubes, is orders of magnitude more viscous than the pure PC even at high frequencies. The masterbatch material exhibits a very strong shear thinning effect; whereas, the neat PC shows only a small frequency dependence. The complex viscosity increases with the nanotube content. The effect of the nanotubes is most pronounced at low frequencies and the relative effect diminishes with increasing frequency due to shear thinning. This is in accordance with theoretical expectations and experimental observations for fiber-reinforced composites [25–27]. It is interesting to note that the viscosity curves for 0.5 and 1 wt% nanotubes have similar frequency dependencies as the pure PC, revealing a Newtonian plateau at low frequencies. However, above 2 wt% nanotubes, the viscosity curves have a much steeper slope at low frequencies, and there is no Newtonian plateau within the frequency range studied. At 5 wt% nanotubes, the rate at which the complex viscosity decreases with frequency is nearly identical to that of the 15 wt% masterbatch, i.e. the viscosity curve is nearly linear over the range of frequencies shown.

Fig. 3 shows the complex viscosity versus nanotube content at different frequencies. At low frequencies, the increase in viscosity is not linear with composition. At 0.1 and 1 rad/s, there is initially a slow rise in viscosity up to 1 wt% nanotubes. This is followed by a steep slope between 1 and 5 wt%; and between 5 and 15 wt% the slope is lower. At high frequencies (100 rad/s), the viscosity increases nearly linearly with the nanotube content. The increase in complex viscosity with nanotube composition is primarily caused by a dramatic increase in the storage modulus G', as may be seen in Fig. 4. The corresponding increase in the loss modulus G'' is much lower as seen in Fig. 5. Both moduli increase with frequency; however, the rate of increase becomes less the higher the nanotube content. Thus, the effect of nanotube concentrations is much higher at low frequencies than at high frequencies. The values of G' and G'' for the composites containing 0.5 and 1 wt% nanotubes, while significantly higher than that of the pure PC, do not differ very much from each other. Above 1 wt%, the slopes of the modulus curves change significantly; however, beyond 5 wt% nanotubes, G' is nearly independent of frequency.

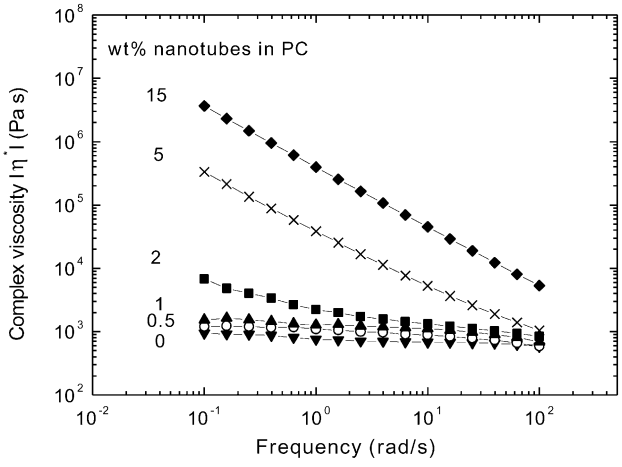

Fig. 2. Complex viscosity of nanotube filled polycarbonate at 260 °C.

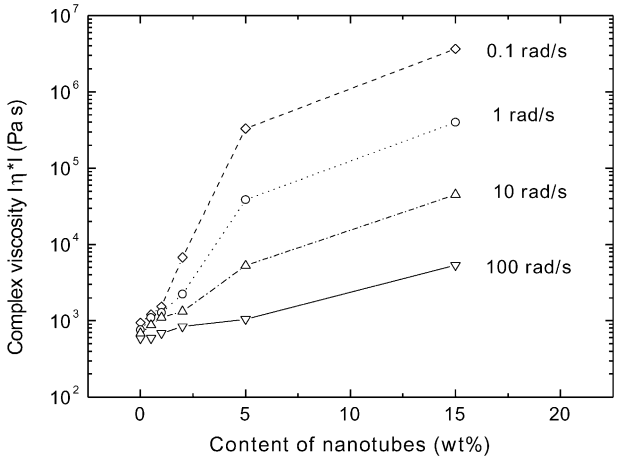

Fig. 3. Complex viscosity versus nanotube content at different frequencies.

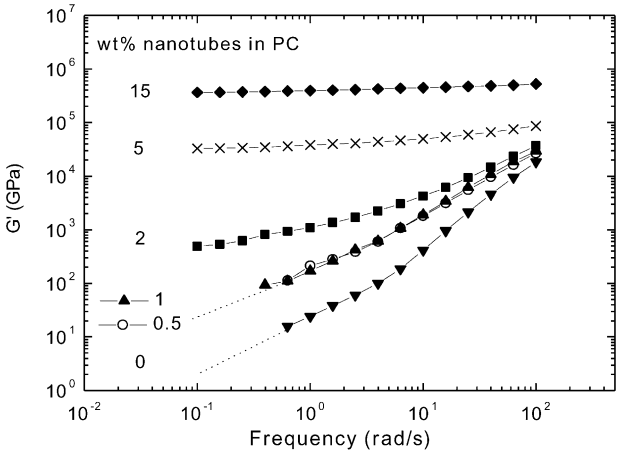

Fig. 4. Storage modulus G' of nanotube filled polycarbonate at 260 °C.

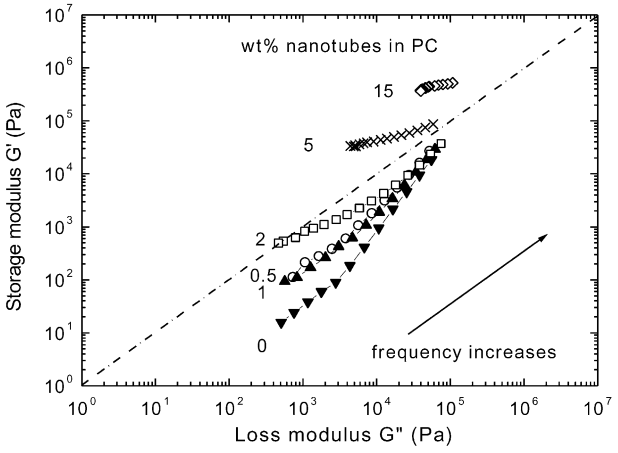

Fig. 6. Storage modulus G' as function of loss modulus G'' of nanotube filled polycarbonate at 260 °C.

It is known from the literature that interconnected structures of anisometric fillers result in an apparent yield stress which is visible in dynamic measurements by a plateau of G' or G'' versus frequency at low frequencies [21,28,29,38]. This effect is more pronounced in G' than in G'' [28]. As the nanotube content increases in this composite system, nanotube–nanotube interactions begin to dominate, eventually lead to percolation and the formation of an interconnected structure of nanotubes. Starting at about 2 wt% nanotubes, G' seems to reach such a plateau at low frequencies. Therefore, an interconnected structure is assumed to form. This critical composition is regarded as a rheological percolation composition. At high concentrations of nanotubes, connectivity is more pronounced, as seen in the enhanced elasticity.

Fig. 6 shows a plot of the storage modulus G' versus the loss modulus G'' with frequency as a parameter; analogous to Cole–Cole plots used in dielectric spectroscopy [30,31]. Such plots were used by Han et al. [32–34] to investigate temperature induced changes in the microstructure of homopolymers, block copolymers and blends. It was proposed that if the microstructure does not change with temperature, curves of $\log G'$ versus $\log G''$ at different temperatures should coincide, as is the case in the single phase melt. When the microstructure changes with temperature, different curves of $\log G'$ versus $\log G''$ are expected. Such plots can also be used to elucidate structure differences at a fixed temperature. For example, Harrell and Nakayama [35,36] used $\log G''$ versus $\log G'$ plots which they called 'modified Cole–Cole plots' to explore the influence of branching and the broadening of the molecular weight distribution of polyethylene on the microstructure. It was shown that at a given G'', G' increases as the degree of long chain branching increased. In multiphase systems, such plots can be used in a similar way to indicate structural differences between the matrix and filled systems at a given temperature. For example, Han and Kim [37] show that increasing the rubber content increases the elastic properties of an acrylonitrile–butadiene–styrene material.

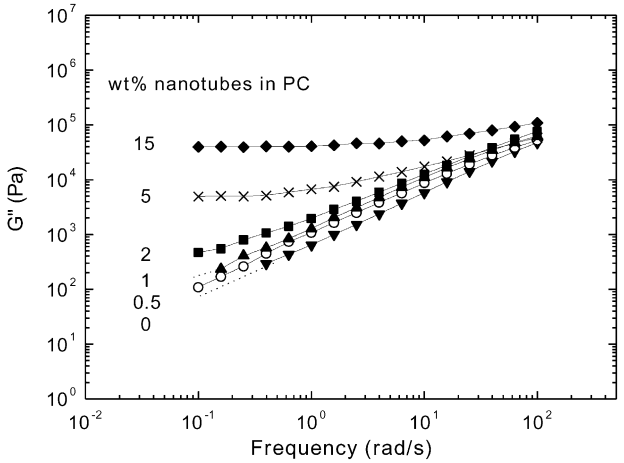

Fig. 5. Loss modulus G'' of nanotube filled polycarbonate at 260 °C.

For the nanocomposites of interest here, the storage modulus, G' (for a given loss modulus, G''), increases significantly with increasing content of nanotubes (Fig. 6). At contents 5 wt% and above, G' is higher than G''. The slope of G' versus G'' decreases with increasing nanotube content. Kitano et al. [27] found a similar response of the first normal-stress difference versus shear stress for glass fiber filled polyethylene melts under steady-state shear conditions. According to Han and Lem [32], there is a qualitative similarity between plots of the first normal-stress difference versus shear stress and plots of G' versus G''. The shift and the change in slope of the G' versus G'' curves indicate that the microstructure of these composites changes significantly with addition of nanotubes.

Figs. 7 and 8 show plots of the storage modulus G' and the loss modulus G'' versus nanotube content at different frequencies. These plots again show that the increase in G' with the nanotube content is much higher than that of G''. The increase with composition is non-linear and is more prominent at concentrations below 5 wt%

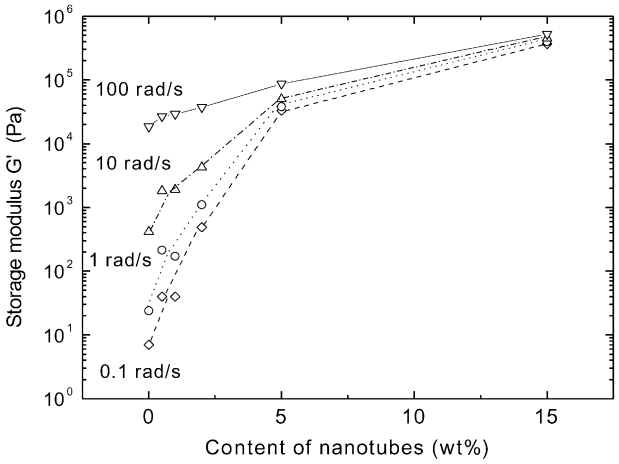

Fig. 7. Storage modulus G' versus nanotube content at different frequencies.

than above. This observation is especially evident at low frequencies.

3.3. Morphology

It was of interest to explore the morphology of the polymer–CNT composites. Fig. 9 shows three SEM photomicrographs of nylon 6 (a) and polycarbonate (b, c) masterbatches containing 20 and 15 wt% nanotubes, respectively. All three images show that the nanotubes are randomly oriented and form interconnecting structures. Due to the complexity of the nanotube network, it is virtually impossible to obtain any information from the SEM photomicrographs about the fiber length. However, an interesting observation can be made concerning the nanotube diameters for each system. As previously mentioned, Hyperion reports that their nanotubes typically range between 10 and 15 nm. The photomicrograph for the nylon 6 system reveals that the diameters are in the range of 10 nm. In contrast, the photomicrographs for the polycarbonate composite show apparent diameters ranging from 10 to 50 nm. The higher observed diameters suggest that an adsorbed layer of polycarbonate exists on the nanotubes. Closer examination of the nanotubes, i.e. in Fig. 9(c), reveals a layer of PC that seems to cover the nanotube surface, indicating some degree of wetting and phase adhesion, unlike the polyamide system.

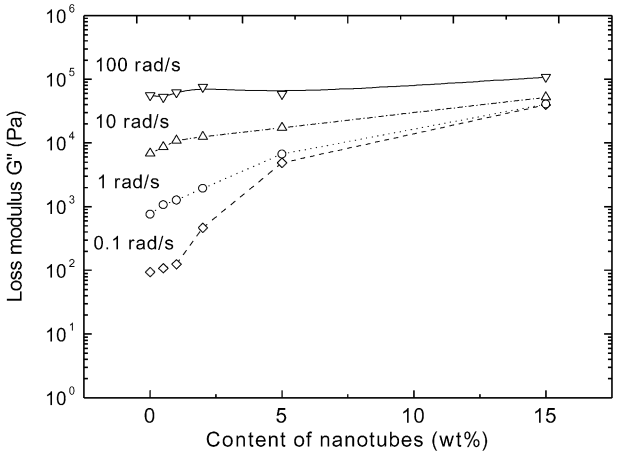

Fig. 8. Loss modulus G'' versus nanotube content at different frequencies.

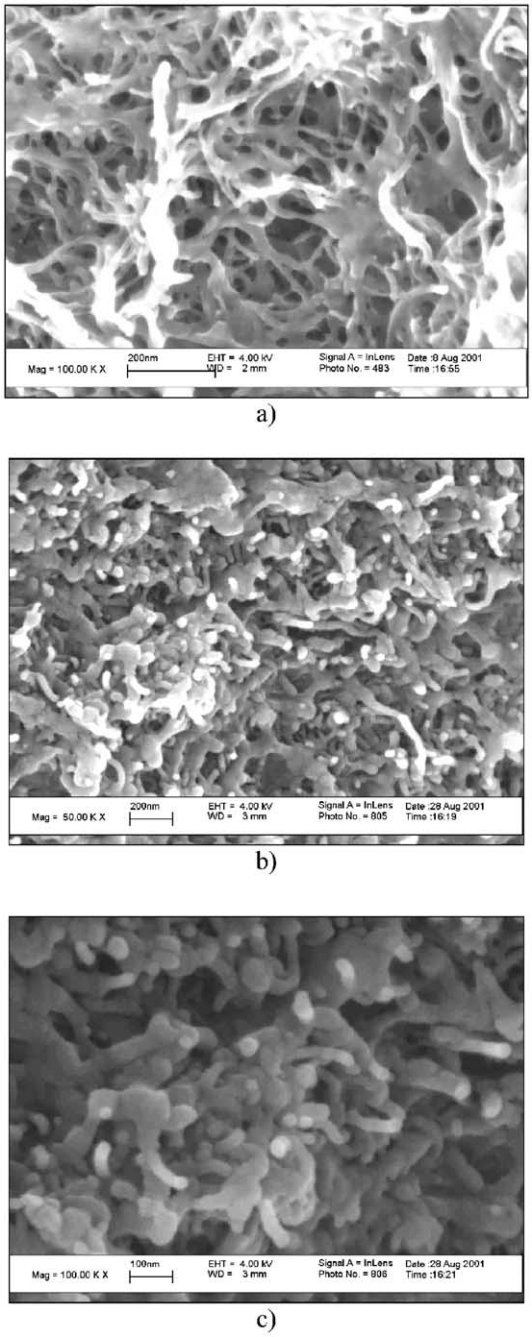

Fig. 9. SEM photomicrographs of fracture surfaces without sputtering: (a) PA6 masterbatch containing 20 wt% CNT; (b) and (c) masterbatch containing 15 wt% CNT.

The cryofracture of composites with 5 wt% nanotubes, Fig. 10, shows that the crack propagates through the matrix

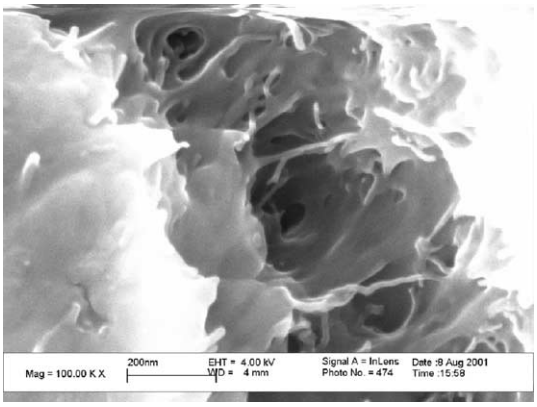

Fig. 10. SEM micrographs of PC + 5 wt% nanotubes, fracture surface, without sputtering.

material but does not necessarily destroy the nanotubes themselves. As in the masterbatch, the nanotubes still appear to be arranged randomly in space. The nanotubes seem to bridge the crack in the matrix. This may be a way to enhance the strength of the composite. Such an effective load transfer mechanism has been described by Jin et al. [15] and Qian et al. [8] for MWNT in thermoplastics and by Ajayan et al. [39] for SWNT in epoxy composites.

Fig. 11 shows a photomicrograph of samples dissolved in THF. Each sample contains the same amount of nanotubes. The solutions made from the lowest concentrated composites, 0.5 and 1 wt% composites (left two vials), have a very dark appearance and are believed to consist predominantly of finely dispersed individual nanotubes. Dissolution of the 2 wt% nanocomposite in THF (middle vial) reveals a noticeable change in appearance. The solution contains finely dispersed nanotubes, corresponding to the overall gray color, and precipitated black particles. The black sediment is believed to be the remains of an interconnected structure of nanotubes. At the percolation threshold, the nanotubes form an interconnecting structure, exhibiting a high degree of particle–particle interactions and/or entanglements. This increased nanotube interaction inhibits complete dispersion of the nanotubes in THF, as seen in the 2 wt% composite vial. Beyond the percolation threshold, nanotube connectivity is more pronounced. This effect is evident in the inhomogeneous solutions pertaining to the 5 and 15 wt% composites (right two vials in Fig. 11). Both vials contain a considerable amount of solid black particles,

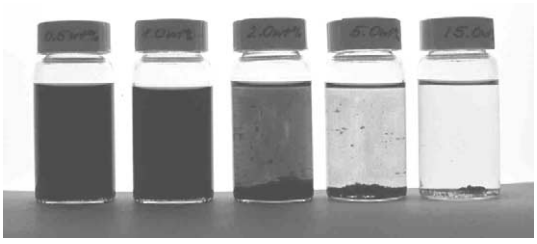

Fig. 11. Dissolving experiments on nanotube filled polycarbonates after 2 weeks in THF, from left to right: 0.5, 1, 2, 5, and 15 wt% composites.

while the liquid phase appears to be nearly transparent. The liquid phases have only a small fraction of free floating individual nanotubes. Instead, the bulk of the nanotubes reside within the black particles, in the form of a highly interconnected structure. In general, the percolation effect seen here supports both electrical and rheological findings.

4. Discussion

4.1. Electrical and rheological percolation thresholds

The results shown above strongly suggest an electrical percolation threshold between 1 and 2 wt% nanotubes in polycarbonate. This threshold is much lower than the 9–18 wt% range reported by Lozano et al. [3,4] for vapor grown carbon nanofibers used as a model for SWNT and MWNT in polypropylene. The reason for this difference is primarily due to the different aspect ratios which are about 100–1000 for the nanotubes used here versus about 10–100 for the fibers used by Lozano et al. A simple relationship between geometrical percolation threshold and aspect ratio was given by Balberg [40]. For randomly distributed cylinders, the critical volume fraction for percolation is proportional to the inverse of the aspect ratio; this suggests the percolation threshold for the thinner nanotubes used here should occur at a concentration about one-tenth of that for the fibers used by Lozano et al. The experimental findings are in reasonable agreement with this calculation.

In addition, the electrical percolation threshold seems to be dependent on the matrix material or process used. Shaffer and Windle [18] reported that poly(vinyl alcohol) composites formed from the same kind of Hyperion nanotubes have a percolation threshold between 5 and 10 wt% nanotube content. Composites based on epoxy resins produced by curing of nanotube dispersions in the liquid precursor were found to exhibit a percolation threshold below 0.04 wt% as described by Sandler et al. [23]. In addition, these composites have a much higher electrical conductivity compared to composites with thermoplastic polymers. Shaffer and Windle [18] attributed these differences to an adsorbed polymer layer around the nanotubes which reduces the quality and quantity of electrical contacts between the nanotubes. On the other hand, such a layer may also be a requirement for high phase adhesion and enhanced mechanical properties.

Interestingly, the observed resistivity threshold occurs in the same concentration range as the increase in melt viscosity found at low frequencies. Starting at 2 wt% nanotubes the frequency dependence of the viscosity curves changed significantly and a step increase in the viscosity–composition relation was observed at low frequencies. This suggests that the rheological behavior can be a tool for identifying the percolation threshold for these composites. This notation agrees with findings by other authors. Lozano et al. [4] reported a melt viscosity threshold for

low frequencies at around 10 wt% nanofibers in PP corresponding to the conductivity threshold. Compositions containing less than 10 wt% nanofibers showed only a small increase in viscosity and followed closely the viscosity–frequency behavior of the unfilled PP. Higher filler contents up to 30 wt% showed a significant increase in viscosity, especially at low frequencies.

4.2. Rheological properties and expected processing behavior

Compared to prior results from the literature, the increase in viscosity with filler content reported here is much higher. The large increase is believed to be caused by the very high aspect ratio of the nanotube fibrils. The comparison of the above results with the results of Lozano et al. [4] indicates that the increase in viscosity at a given fiber content is strongly dependent on the aspect ratio of the filler. Similar results were found by Kitano et al. [27] for polyethylene melts filled with glass fibers. The viscosity increase at a given fiber concentration was higher the larger the aspect ratio; this was quite pronounced at low shear rates. However, the increase in viscosity at the threshold composition relative to the pure matrix in the present system seems to be in about the same range as the relative increase in viscosity shown by Lozano et al. [4] at their respective threshold composition.

At high frequencies, characteristic of processing behavior, the viscosity is only slightly changed by adding up to 5 wt% nanotubes. Thus, composites around the percolation threshold are expected to have about the same processing behavior as the neat polymer in practical applications. However, we have to consider that the Cox–Merz rule may fail in filled systems. For highly filled wollastonite–polypropylene systems [21], it was found that the steady-state data measured at low shear rates, e.g. below 1 s^{-1}, were consistently higher than the dynamic data. The difference increased with increasing loading (up to 60 phr) and was considered to be caused by predominantly higher particle–particle interactions under steady-state conditions. On the other hand, at higher shear rates orientation of anisometric plate-like fillers may lead to lower viscosities in capillary flow regimes as mentioned by Fornes et al. [41] for organoclay nanocomposites based on polyamide 6. Whether such significant differences also exist in composites with low nanotube contents should be explored in future investigations. Hagerstrom and Greene [6][2] reported that low nanotube loadings facilitate higher melt flow in composites as compared to other types of conductive fillers which require much higher concentration to achieve the conductivity threshold (e.g. carbon fibers). Hagerstrom et al. point out that this is a significant advantage for thin wall molding applications.

It should be emphasized that the composites investigated here were obtained by compression molding, a technique that typically results in a relatively random distribution of fibers. In injection molded samples, which are more commonly encountered in practical applications, some degree of orientation of the nanotubes in the flow direction is possible. With this in mind, the percolation threshold may be somewhat different from that observed here for compression molded samples.

5. Summary and conclusions

The rheological behavior of compression molded mixtures of polycarbonate and CNTs were investigated using oscillatory rheometry at a constant temperature of 260 °C. The nanotubes have a diameter of about 10–15 nm and lengths in the range 1–10 μm. The viscosity increases significantly with increasing nanotube concentration. The viscosity of these composites was shown to be significantly dependent upon test frequency. Pure polycarbonate and composites containing less than 2 wt% CNT show similar frequency dependencies and reach a Newtonian plateau at low frequencies. Above 2 wt% nanotubes, the viscosity curves exhibit a much greater decrease with frequency and exhibit non-Newtonian behavior to much lower frequencies. Therefore, 2 wt% may be regarded as a rheological threshold composition. The viscosity increase is accompanied by an increase in the elastic melt properties, represented by the storage modulus G', which is much higher than the increase of the loss modulus G''.

Ultimately, the rheological threshold coincidences with the conductivity percolation threshold which was found to be between 1 and 2 wt%. This indicates that the rheological response is sensitive to the interconnectivity of the nanotubes, which is also directly related to electrical conductivity.

The increase in viscosity with composition is much higher than reported for nanofibers having higher diameters and for carbon black composites. This difference is caused by the higher aspect ratio of the nanotubes used. Interestingly, the relative viscosity increase at the threshold composition is about the same range as reported for nanofibers with lower aspect ratio.

Acknowledgements

The authors are grateful for the financial support granted by the Max-Kade-Foundation (New York) to P.P. We would also like to thank Hyperion Catalysis International for providing the masterbatch materials and Prof. Peter F. Green for use of the ARES rheometer.

References

[1] Subramoney S. Adv Mater 1998;10(15):1157–71.
[2] Haggenmueller R, Gommans HH, Rinzler AG, Fischer JE, Winey KI. Chem Phys Lett 2000;330:219–25.
[3] Lozano K, Barrera EV. J Appl Polym Sci 2001;79:125–33.

[4] Lozano K, Bonilla-Rios J, Barrera EV. J Appl Polym Sci 2001;80:1162–72.
[5] Jin Z, Pramoda KP, Xu G, Goh SH. Chem Phys Lett 2001;337:43–47.
[6] Hagerstrom JR, Greene SL. Electrostatic dissipating composites containing hyperion fibril nanotubes. Commercialization of Nanostructured Materials, Miami, USA, April 7, 2000.
[7] Ferguson DW, Bryant EWS, Fowler HC. ESD thermoplastic product offers advantages for demanding electronic applications, ANTEC'98, 1998. p. 1219–22.
[8] Qian D, Dickey EC, Andrews R, Rantell T. Appl Phys Lett 2000;76(20):2868–70.
[9] Schadler LS, Giannaris SC, Ajayan PM. Appl Phys Lett 1998;73(26):3842–4.
[10] Salvetat JP, Briggs GAD, Bonard JM, Bacsa RR, Kulik AJ, Stöckli T, Burnham NA, Forró L. Phys Rev Lett 1999;82(5):944–7.
[11] Walters DA, Ericson LM, Casavant MJ, Lui J, Colbert DT, Smith KA, Smalley RE. Appl Phys Lett 1999;74(25):3803–5.
[12] Li F, Cheng HM, Bai S, Su G, Dresselhaus MS. Appl Phys Lett 2000;77(20):3161–3.
[13] Wildöer JWG, Venema LC, Rinzler AG, Smalley RE, Dekker C. Nature 1998;391:59–62.
[14] Odom TW, Huang JL, Kim P, Lieber C. Nature 1998;391:62–4.
[15] Jin L, Bower C, Zhou O. Appl Phys Lett 1998;73(9):1197–9.
[16] Stéphan C, Nguyen TP, Lamy de la Chapelle M, Lefrant S, Journet C, Bernier P. Synth Met 2000;108:139–49.
[17] Bower C, Rosen R, Jin L, Han J, Zhou O. Appl Phys Lett 1999;74(22):3317–9.
[18] Shaffer MSP, Windle AH. Adv Mater 1999;11(11):937–41.
[19] Coleman JN, Curran S, Dalton AB, Davey AP, Mc Carthy B, Blau W, Barklie RC. Synth Met 1999;102:1174–5.
[20] Lamy de la Chapelle M, Stéphan C, Nguyen TP, Lefrant S, Journet C, Bernier P, Munoz E, Benito A, Maser WK, Martinz MT, de la Fuente GF, Guillard T, Flamant G, Alvarez L, Laplaze D. Synth Met 1999;103:2510–2.
[21] Shenoy AV. Rheology of filled polymer systems. Dordrecht: Kluwer Academic Publishers, 1999.
[22] Shaffer MSP, Fan X, Windle AH. Carbon 1998;36(11):1603–12.
[23] Sandler J, Shaffer MSP, Prasse T, Bauhofer W, Schulte K, Windle AH. Polymer 1999;40:5967–71.
[24] Cho JW, Paul DR. Polymer 2001;42:1083.
[25] Mutel AT, Kamal MR. Rheological properties of fiber-reinforced polymer melts. In: Utracki LA, editor. Two phase polymer systems. Munich: Carl Hanser, 1991. p. 305–31, Chapter 12.
[26] Kitano T, Kataoka T. Rheol Acta 1980;19:753–63.
[27] Kitano T, Kataoka T, Nagatsuka Y. Rheol Acta 1984;23:20–30.
[28] Utracki LA. Polym Compos 1986;7:274.
[29] Utracki LA. Rheology and processing of multiphase systems. In: Ottenbrite RM, Utracki LA, Inoue S, editors. Current topics in polymer science, rheology and polymer processing/multiphase systems, vol. II. Munich: Carl Hanser, 1987. p. 7–59.
[30] Cole KS, Cole RH. J Chem Phys 1941;9:341.
[31] Havriliak Jr. S, Havriliak SJ. Dielectric and mechanical relaxation in materials: analysis, interpretation, and application to polymers. Munich: Hanser, 1997.
[32] Han CD, Lem KW. Polym Engng Rev 1983;2:135–65.
[33] Chuang HK, Han CD. J Appl Polym Sci 1984;29:2205–29.
[34] Han CD, Kim J, Kim JK. Macromolecules 1989;22:383–94.
[35] Harrell ER, Nakayama N. J Appl Polym Sci 1984;29:995–1010.
[36] Nakayama N, Harrell ER. Modified Cole–Cole plot as a tool for rheological analysis of polymers. In: Ottenbrite RM, Utracki LA, Inoue S, editors. Current topics in polymer science, rheology and polymer processing/multiphase systems, vol. II. Munich: Carl Hanser, 1987. p. 149–65.
[37] Han CD, Kim J. J Polym Sci: B Polym Phys 1987;25:1741–64.
[38] Dealy M, Wissbrun KF. Melt rheology and its role in plastic processing theory and application. Dordrecht: Kluwer Academic Publishers, 1999.
[39] Ajayan PM, Schadler LS, Giannaris C, Rubio A. Adv Mater 2000;12(10):750–3.
[40] Balberg I. Phil Mag B 1987;56:991–1003.
[41] Fornes TD, Yoon PJ, Keskkula H, Paul DR. Polymer 2001;42(25):9929–40.